A comparison of standard migration with EOM for Hussar data

Thais A. Guirigay, John C. Bancroft, and J. Helen Isaac

ABSTRACT

Equivalent Offset Migration (EOM) is a method of prestack time migration based on the principles of prestack Kirchhoff migration and its advantages are simpler, faster, flexible and more reliable than the conventional methods.

Common Scatter gathers are created for each output migrated trace based on the EOM method. The gathers have high fold and offsets that can be greater than the maximum source-receiver offset. This high fold and large offsets provides a better focus of the semblance plot, and therefore improves the resolution of velocity analysis over conventional common midpoint gathers. The estimated velocity is RMS type, independent of dip. After velocity analysis, normal moveout and stacking completes the prestack migration.

Prestack time migration requires an accurate velocity model for get a good image of the subsurface.

The intent of this paper is to provide a comparison between a standard poststack time migration or prestack time migration with Equivalent Offset Migration for a data set from Hussar area in Alberta.

INTRODUCTION

Migration is one of the most important processes of the seismic processing and it is used to move event to their positions in time and space. In practice, migration of seismic data requires decision making with regard to an appropriate migration strategies, migration algorithms, and appropriate parameter of the algorithms, migration velocities and issue concerning the input data. Strategies include 2D versus 3D migration, poststack versus prestack migration, and time versus depth migration.

The objective of this paper is to apply two different strategies of migration to seismic data from Hussar, Alberta data set and understand the difference between them. Prestack time migration (PSTM) using Kirchhoff algorithm and Equivalent Offset (EOM) were applied to the data set.

Kirchhoff Prestack Migration concepts

The purpose of migration is to construct an image of the subsurface from seismic reflection data. Prestack migration is a direct process that moves each input sample into all the possible reflection positions, and invokes the principles of constructive and destructive interference to recreate the actual image. All traces are searched to find energy that contributes to the output sample.

Kirchhoff prestack migration is based on a model of the subsurface as an organized set of scattered points. The model assumes that energy may come from a source located anywhere on the surface to all receivers. The location of energy on a recorded trace is the total travel time along the ray path from the source down to the scatter point and back up to the receiver. Kirchhoff prestack migration assumes an output location, and then sums the appropriate energy from all available input traces.

The surface position of a vertical array of scatter points is referred to as the common scatter point (CSP) location. The collection of all input traces that record energy from a given scatter point is referred as the migration aperture. Input traces with energy from a common scatter location can be collected into CSP gathers. This CSP gathers are similar in function to the CMP gathers of conventional processing. (Bancroft et al., 1994)

From the raypaths showed in Figure 1, the traveltime t is estimated by the adding the time from the source to the scatter point t_s and time from the scatter point to the receiver t_r, or

$$t = t_s + t_r. \tag{1}$$

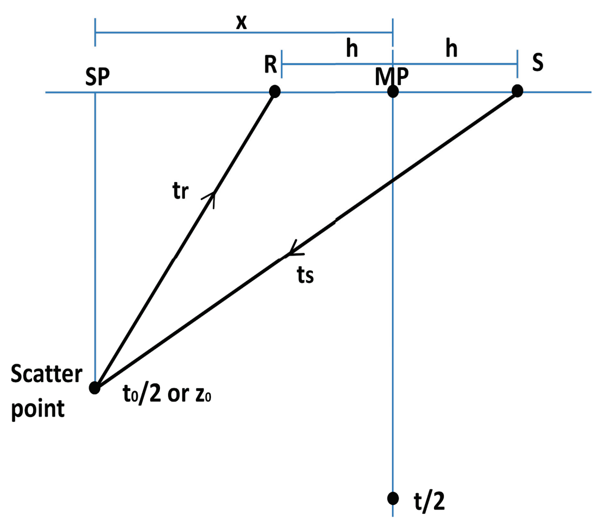

FIG. 1. Geometry of Kirchhoff prestack time migration with source S and receiver R. The total traveltime is the sum of source to scatterpoint t_s and the scatterpoint to receiver time t_r. Taken from Bancroft et al. 1998.

From the geometry, the total or two-way, travel time can be computed from:

$$t = \left[\left(\frac{t_0}{2}\right)^2 + \frac{(x+h)^2}{V_{mig}^2}\right]^{1/2} + \left[\left(\frac{t_0}{2}\right)^2 + \frac{(x-h)^2}{V_{mig}^2}\right]^{1/2}, \tag{2}$$

where x is the location of the source-receiver midpoint (MP) relative to the scatter point (SP) located at $x = 0$, and V_{mig} is the RMS migration velocity evaluated at t_0. The time $t_0 = t\ (x = 0, h = 0)$ is the two-way zero-offset time and t_o is defined from the data.

The equation (2) is known as the double square root (DSR) equation and defines the traveltime surface over which the Kirchhoff summation or integration takes places.

Equivalent Offset Migration

The equivalent offset is defined by converting the DSR equation (2) into an equivalent single square root or hyperbolic form (Bancroft et al., 1998). This can be reformulated by defining a new source and receiver collocated at the equivalent offset position E as illustrates Figure 2. For convenience, the CSP gather is located at $x = 0$. The equivalent offset h_e is chosen to maintain the same traveltime from equation (1):

$$\mathrm{t} = 2\mathrm{t_e} = \mathrm{t_s} + \mathrm{t_r}. \tag{3}$$

This traveltimes can be written as:

$$2\left[\left(\frac{t_0}{2}\right)^2 + \frac{h_e^2}{V_{mig}^2}\right]^{1/2} = \left[\left(\frac{t_0}{2}\right)^2 + \frac{(x+h)^2}{V_{mig}^2}\right]^{1/2} + \left[\left(\frac{t_0}{2}\right)^2 + \frac{(x-h)^2}{V_{mig}^2}\right]^{1/2}. \tag{4}$$

This equation may be solved for the equivalent offset *he* to get:

$$h_e^2 = x^2 + h^2 - \left(\frac{2xh}{tV_{mig}}\right)^2. \tag{5}$$

The equivalent offset is a quadratic sum of the distance *x* between the CSP and the CMP, and *h*, the source-receiver half offset.

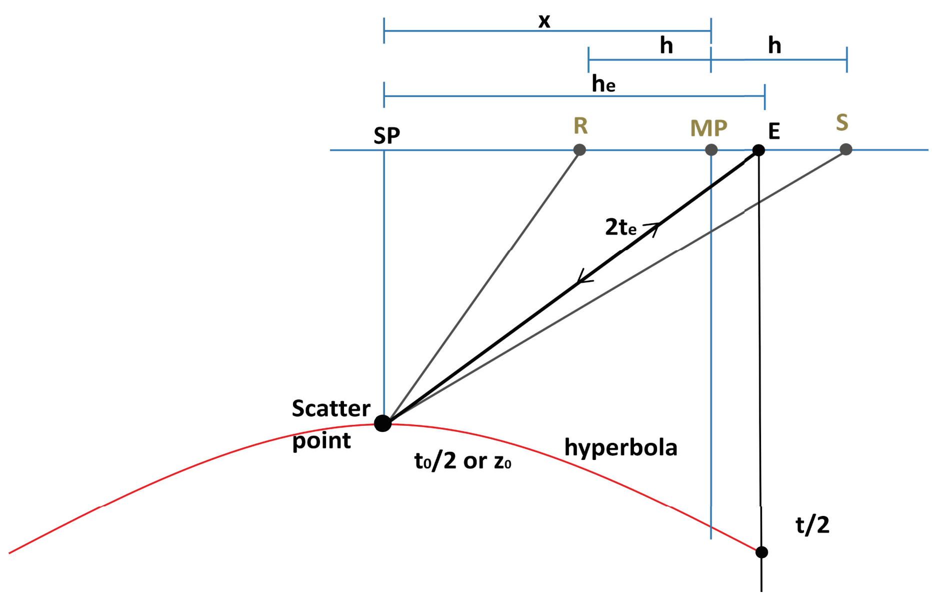

FIG. 2. Equivalent offset h_e is defined as the offset from the surface to a collocated source-receiver having h_e same traveltime as the original source-receiver. Scattered energy from all source pairs lies along the hyperbola at their equivalent offset. Taken from Bancroft et al., 1998.

Equivalent offset migration forms prestack migration gathers, called scatter points (CSP) gathers. Reflection energy in the CSP gathers is hyperbolic with RMS type velocity. (Bancroft, 1995)

After the CSP gathers have been formed, the filtering, scaling, and time shifting, collapse the energy on the CSP gather to zero offset to form a prestack migrated trace.

The gathers have high fold and offsets that can be greater than the maximum source-receiver offset. This high fold improves the resolution of velocity analysis over conventional CMP gathers. After velocity analysis, normal-moveout (NMO) and stacking completes the prestack migration. EOM result will be the same result as prestack Kirchhoff time migration, but with shorter run times. (Bancroft, 1995)

DATA

Hussar seismic survey was acquired in September 2011 by CREWES and the collaboration of Husky Energy, GeoKinetics and Inova, near Hussar, Alberta. The survey was designed to test the use of different sources and receivers to investigate the extension of the seismic bandwidth in the low frequency range.

The acquisition was shot with dynamite and vibroseis and five different types of receivers. Three different vibroseis sources were tested: INOVA's AHV_IV model 363 with custom low-dwell sweep, INOVA's AHV_IV model 360 with linear sweep, and a conventional Failing vibrator with custom low-dwell sweep. The receivers used were: Vectorseis 3C accelerometers, 10 Hz Sensor SM7 3C geophones, 4.5 Hz Sunfull 1C geophone, and Nanometrics seismeters combined with 50 ION-Sensor 10 Hz SM24 high-sensitivity 1C geophones.

A total of 20 volumes of 2D seismic were acquired, with the combination of the three different sources and receivers.

The analysis to be showed in this paper used the data set acquired with 265 shots at 20 meters interval, using INOVA AHV-IV model 364 (Figure 3) , and 224 receives at 20 meters interval with 4.5 Hz Sunfull 1C geophones (Figure 4). The line length was about of 4480 meters. The low-dwell sweep moved slowly through the low frequencies at reduced power and then move linearly through the normal (10-100 Hz) frequency range. (Margrave, 2011)

FIG. 3. INOVA AHV-IV model 364

FIG. 4. Planted 4.5 Hz Sunfull 1C geophone

DATA PROCESSING

The data was processed with a standard flow: geometry, first breaks, statics, elevation statics, geometry spreading compensation, noise attenuation using Radial filter, and deconvolution, using ProMAX software from Landmark. The data was processed to a flat datum at the mid surface elevation.

This data was the input to the Equivalent Offset Migration (EOM) in MATLAB, which generated CSP gathers.

The CSP gathers are in the same plane as the CMP gathers, but contains information from all traces within the migration aperture. The offset in a CDP gather is limited to the maximum source-receiver offset. In contrast, the CSP gather will include all traces within the migration aperture, which can be much larger than the maximum source-receiver offset (Bancroft et al., 1994). Figure 5 shows a two sided CDP gather at the same location as a CSP gather in Figure 6. The CSP gathers contains much high fold and show more coherence energy than the CMP.

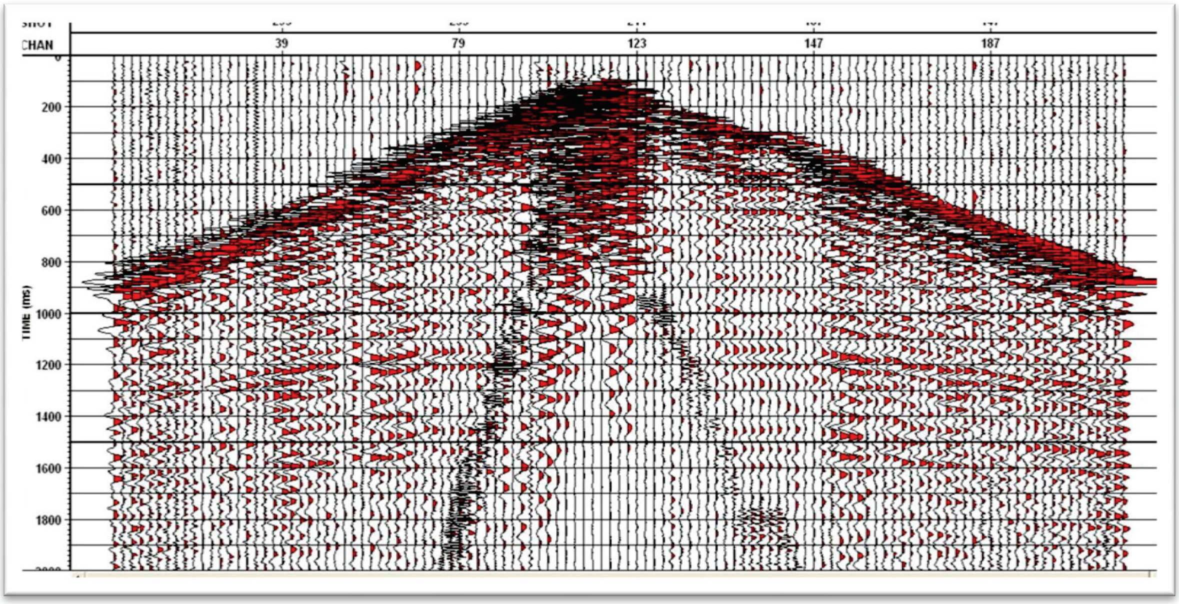

FIG. 5. Two-sided CMP gather at 451

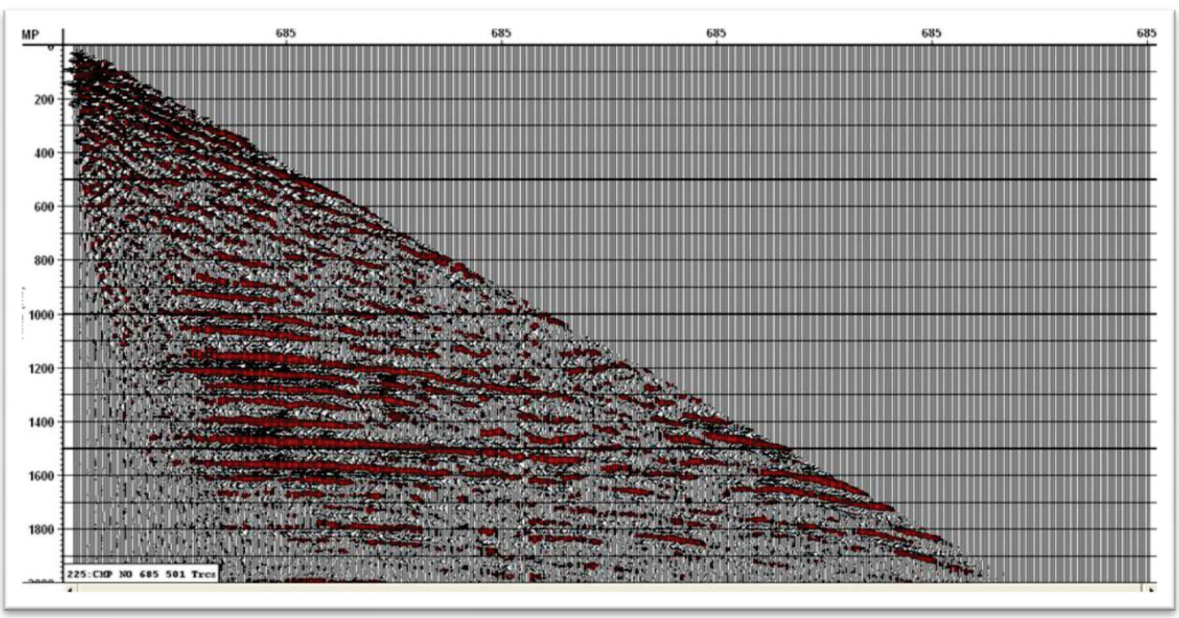

FIG. 6. One side CSP gather at 451

Velocity analysis

The velocity analysis was done for both data sets: one for the original data set, and the other one for the data after Equivalent Offset Migration.

Because the offset of the CSP gathers have higher fold and larger offsets, the velocities on semblance plots focus to smaller points than on conventional semblance plots formed from a CMP gather. Figure 7 shows semblance plots for some CDP's. Figure 8 shows the semblance analysis for CSP gathers at the same CMP location.

The CSP gathers were formed with zero velocity information, and the gathers show better grouping of the energy.

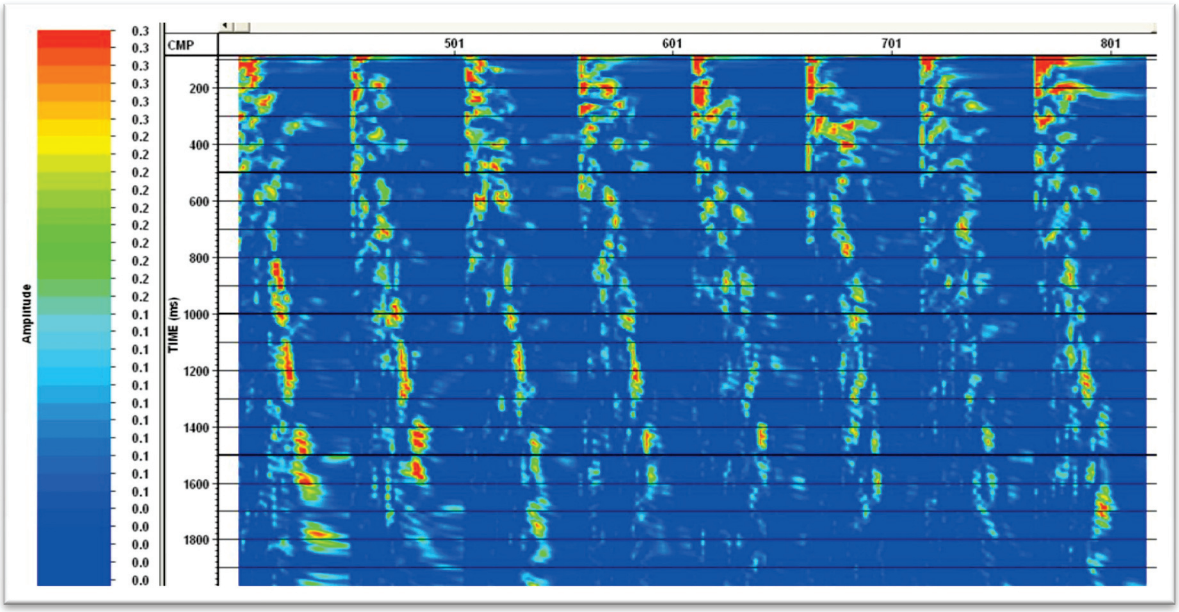

FIG. 7. Semblance display for the CDP's 451, 501, 551, 601, 651, 701, 751 and 801

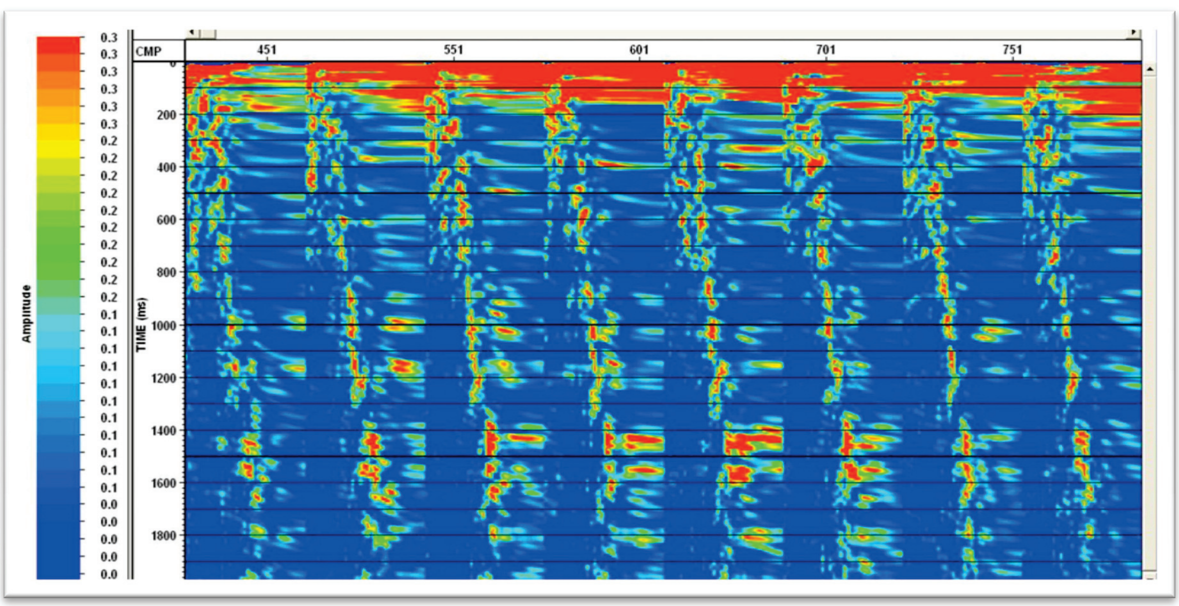

FIG. 8. Semblance analysis for the CSP's 451, 501, 551, 601, 651, 701, 751 and 801

Data without EOM

Figure 9 shows the two-sided CDP 551 before and after the application of NMO, and after the stretch mute.

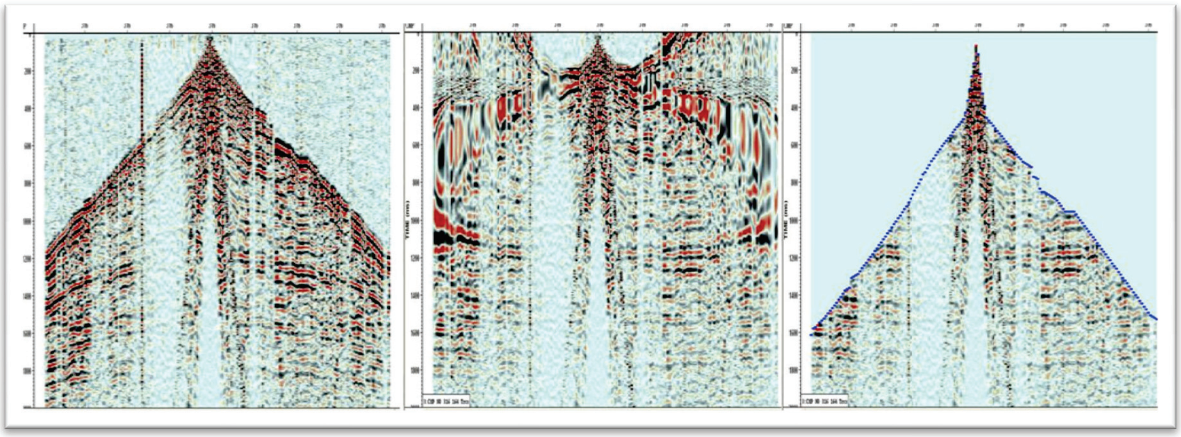

a) b) c)

FIG. 9 Two-sided CDP 551 before a), after apply NMO b), and after stretch mute c).

Different stack sections were generated using different velocity models. Figure 10 shows a stack section using the same constant velocity used for the EOM data. This section shows a low signal noise in the upper part of the section and good reflectors after the middle part of the section. These reflectors show some discontinuities.

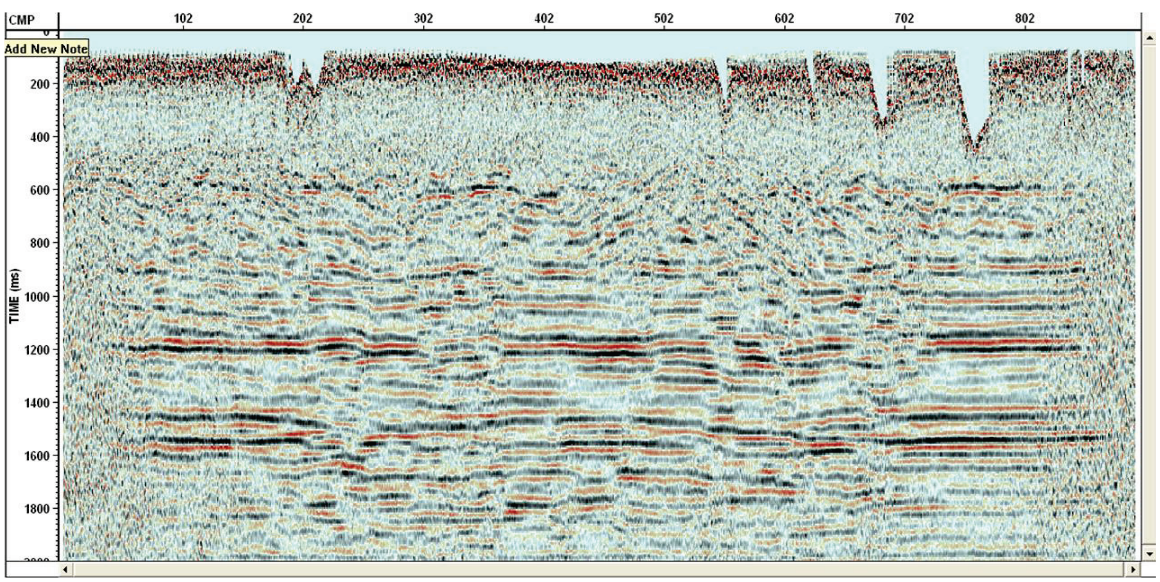

FIG. 10. Stacked section using constant velocity field.

Figure 11 shows the velocity field across the line and Figure 12 shows the stacked section generated using these velocities. This section shows a better image than the section with constant velocities. The reflectors are more continuous than the previous section. (Figure 10)

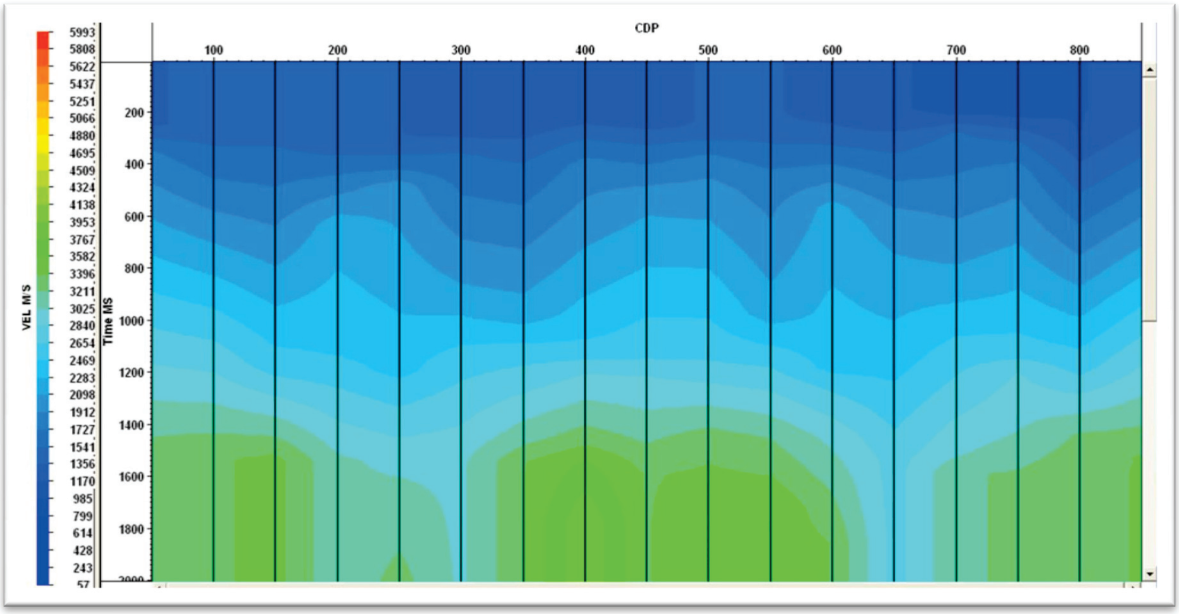

FIG. 11. Velocity analysis over the CMP's

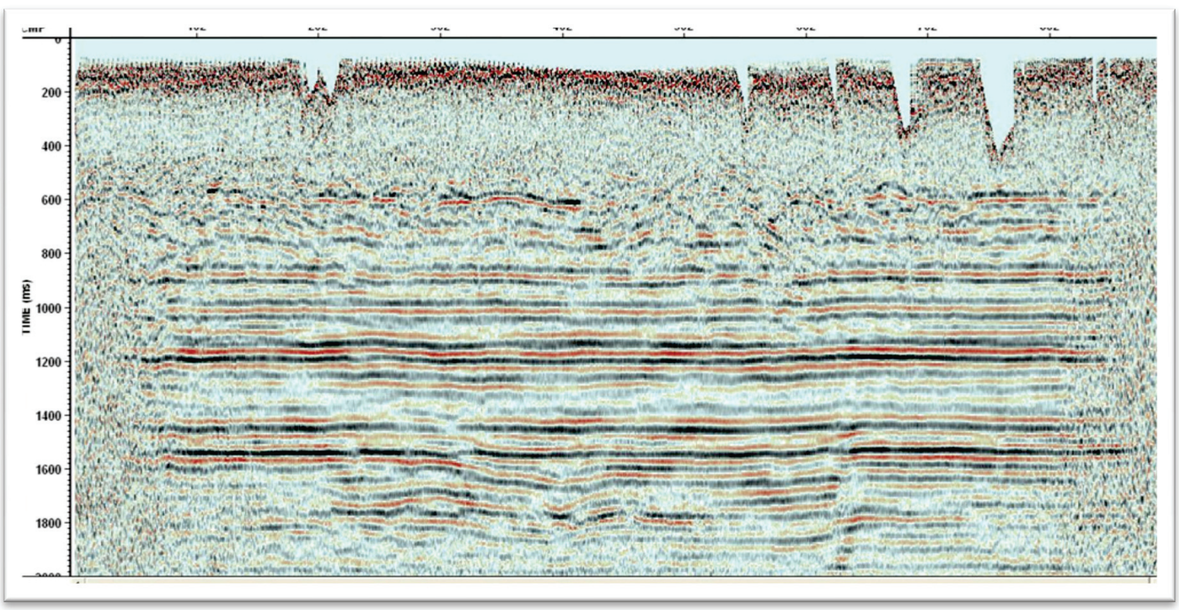

FIG. 12. Final stacked section of Hussar area

Data with EOM

This seismic volume was very sensitive to velocities. The first analysis of velocities (Figure 13) shows the velocity field across the line. This velocity field was used to get a stacked section (Figure 14) and this section shows some features that could had been interpreted as a graben around 1800 msec and between CMP 536 and 636.

To evaluate if this feature was real or not, we did a second velocity analysis and the structure was not observed. We decided to apply constant spatial velocity *V (t)*, using the second velocity at CMP 600 and extend it across the line, because is well known that the area is not geologically complex and the layers are very flat. This constant velocity works very well for the stacked section. Figure 15 shows the second velocity analysis, Figure 16 shows the constant velocity *V(t)* used to stack the line, and Figure 17 shows the stacked seismic section.

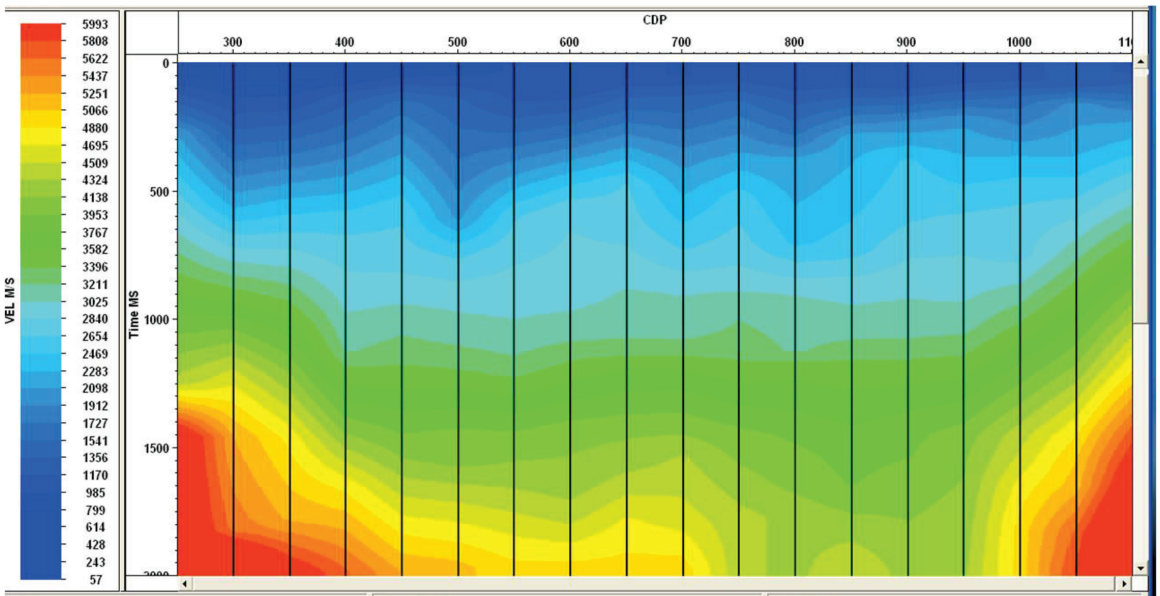

FIG. 13. First velocity analysis over the CSP's

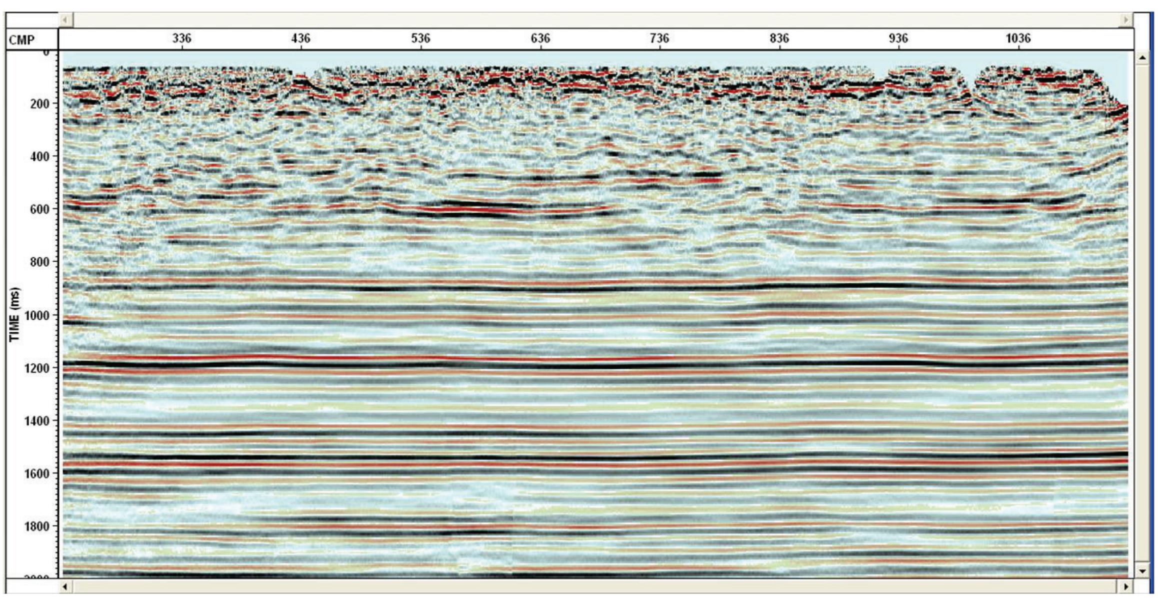

FIG. 14. EOM that was stacked using the first velocity analysis

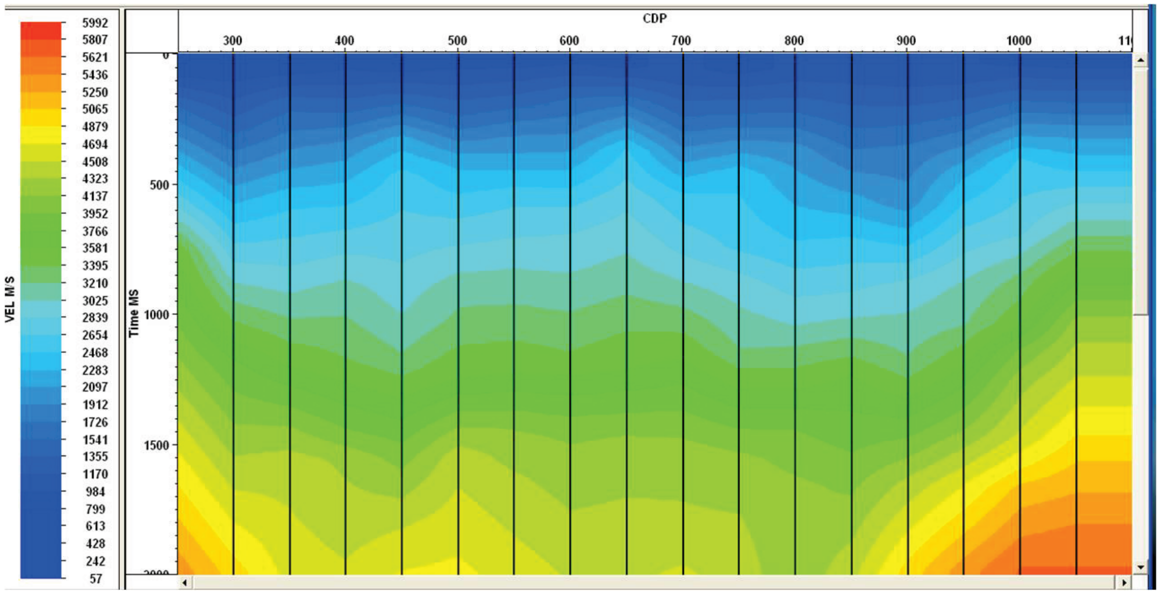

FIG. 15. Second velocity analysis over the CSP's

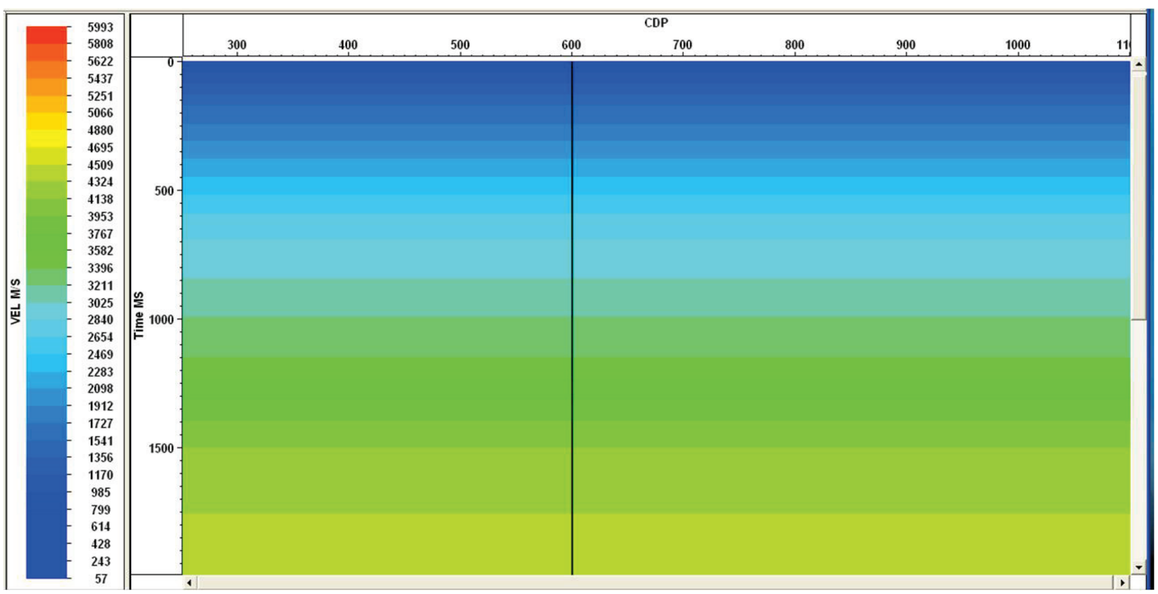

FIG. 16. Constant Velocity field, *V(t)*

The percentage stretch mute also was considered in the seismic processing. Figure 18 shows the analysis of different percentage of stretch mute on equivalent offset (EO) gathers with NMO at CSP 450. These mute are too blocky to use with the NMO, therefore we decided to design different mute curves.

The picture 19 shows the CSP 551 before and after the application of NMO. Note the effect of the stretch moveout over the CSP.

Figure 20 shows five design mute curves for CSP 551. They were designed from short offset to large offset, and one combined curve

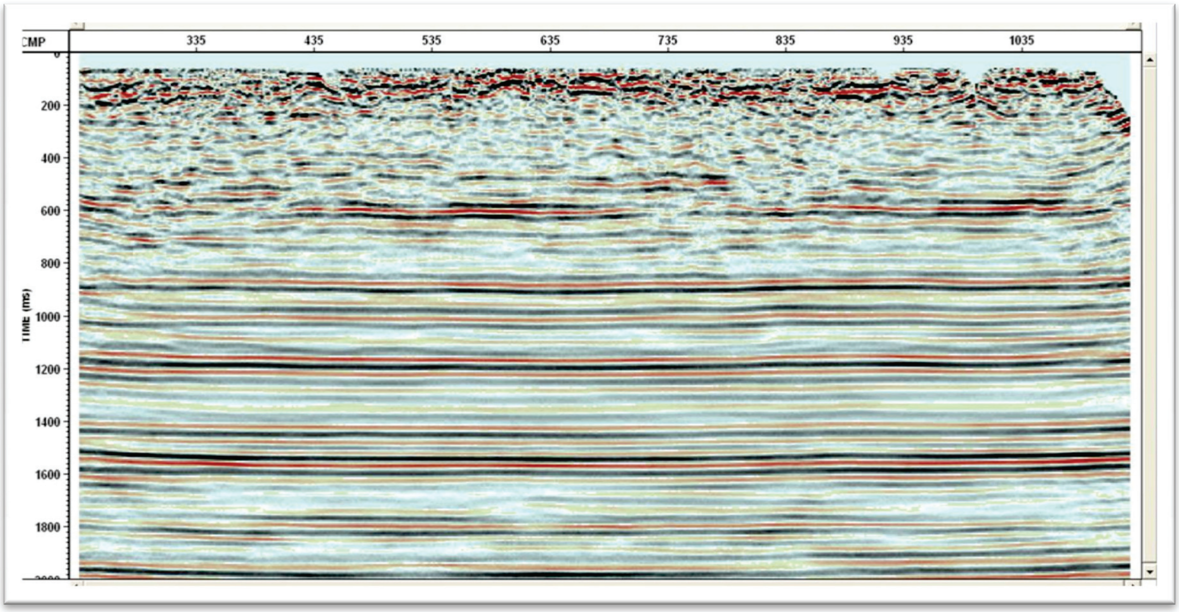

FIG. 17. EOM stacked with *V(t)*

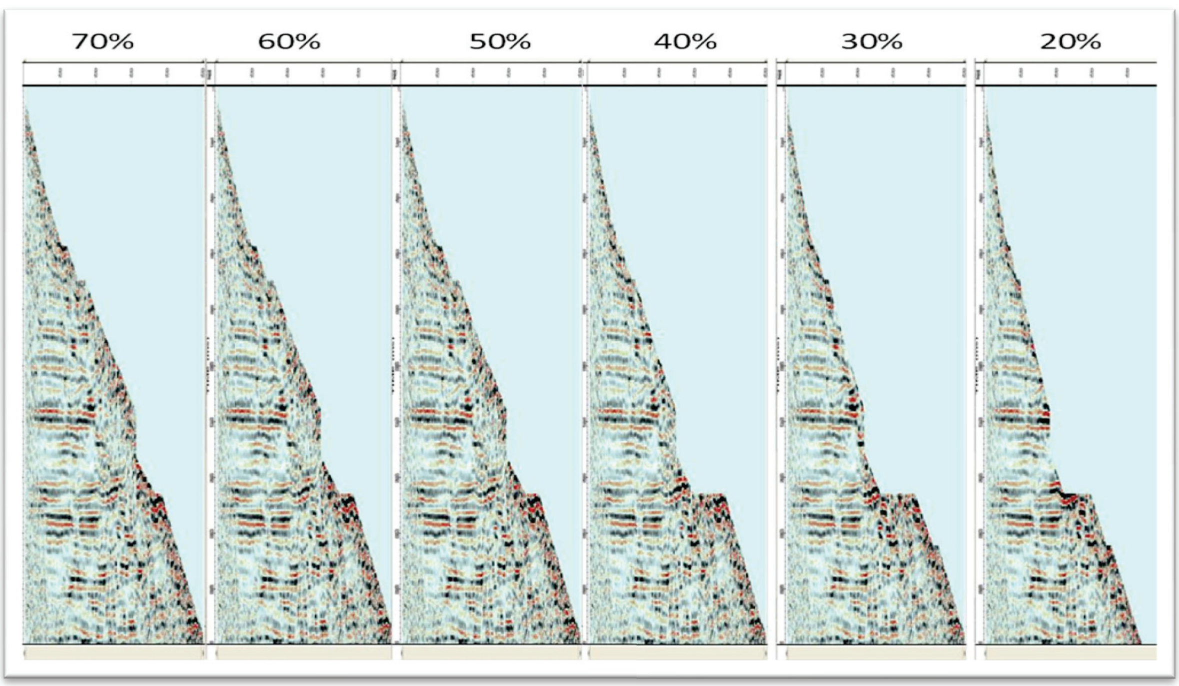

Fig. 18. Different percentage of stretch mute on EO gathers at CSP 450 with NMO applied.

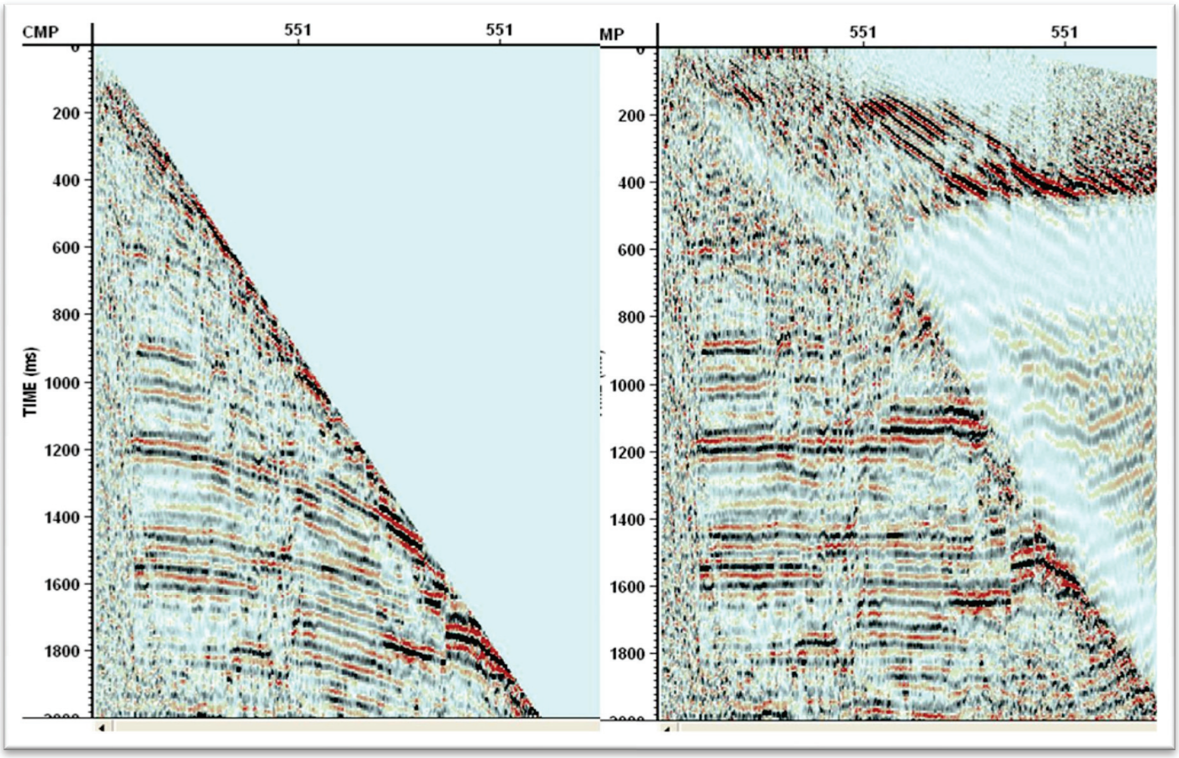

a) b)

FIG. 19. CSP 551 before and after apply NMO.

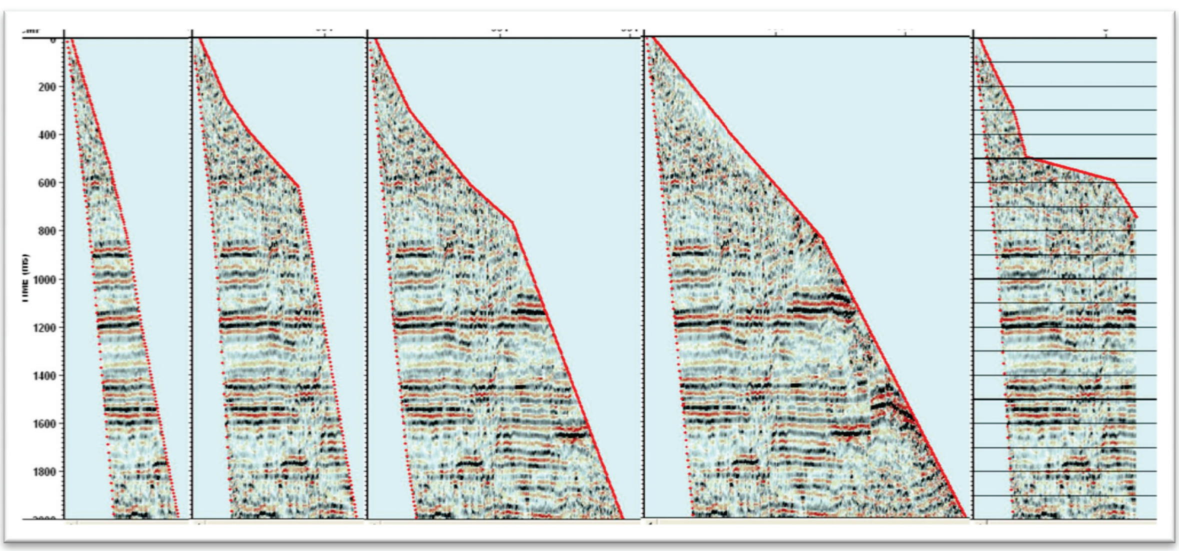

a) b) c) d) e)

FIG. 20. Four design curves for stretch mute NMO at CSP 551. From short offset through large offset a) to d), and combined e).

Figure 21 shows the stacked seismic section using stretch mute with the curve designed called combined, and constant velocity function *V(t)* explained previously. This section is the final stack generated with equivalent offset migration to the data. Now, we are going to compare this result with PSTM Kirchhoff algorithm.

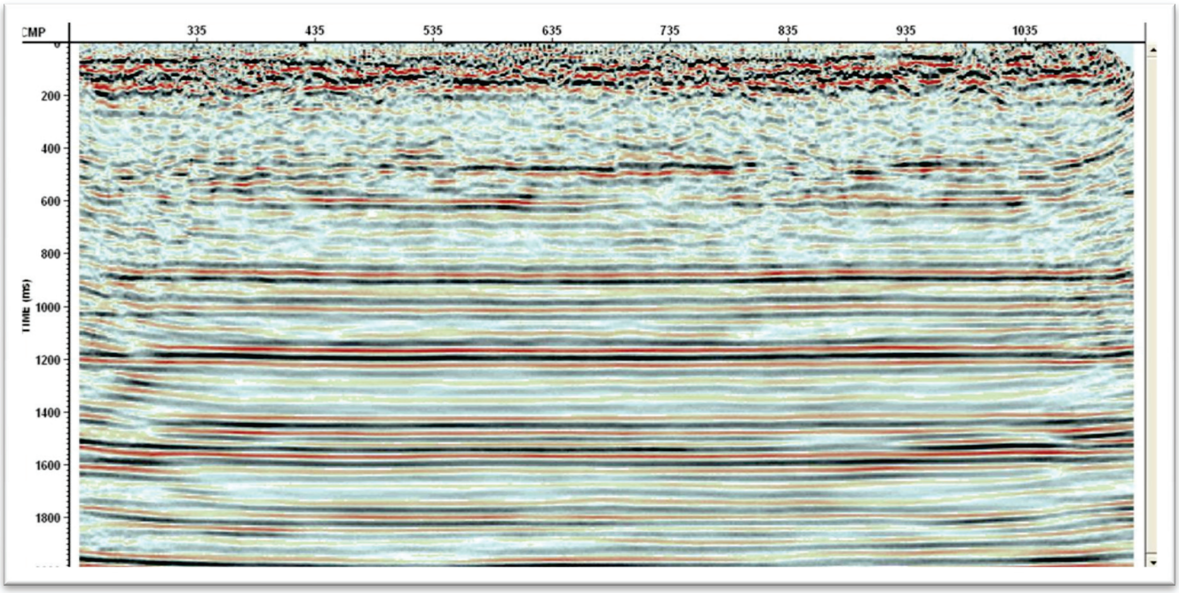

FIG. 21. Stacked section which used the function *V(t)* and combined curve for stretch NMO.

Discussion

The following figures show three different migrations applied to the stacked data shown in Figure 12. Figure 22 shows a section after applied PSTM Kirchhoff. The comparison between two migrated sections: one with EOM (Figure 21) and the other with PSTM Kirchhoff (Figure 22) is that they look completely different. EOM section shows continuous and flat reflectors, while PSTM Kirchhoff shows significant faulting.

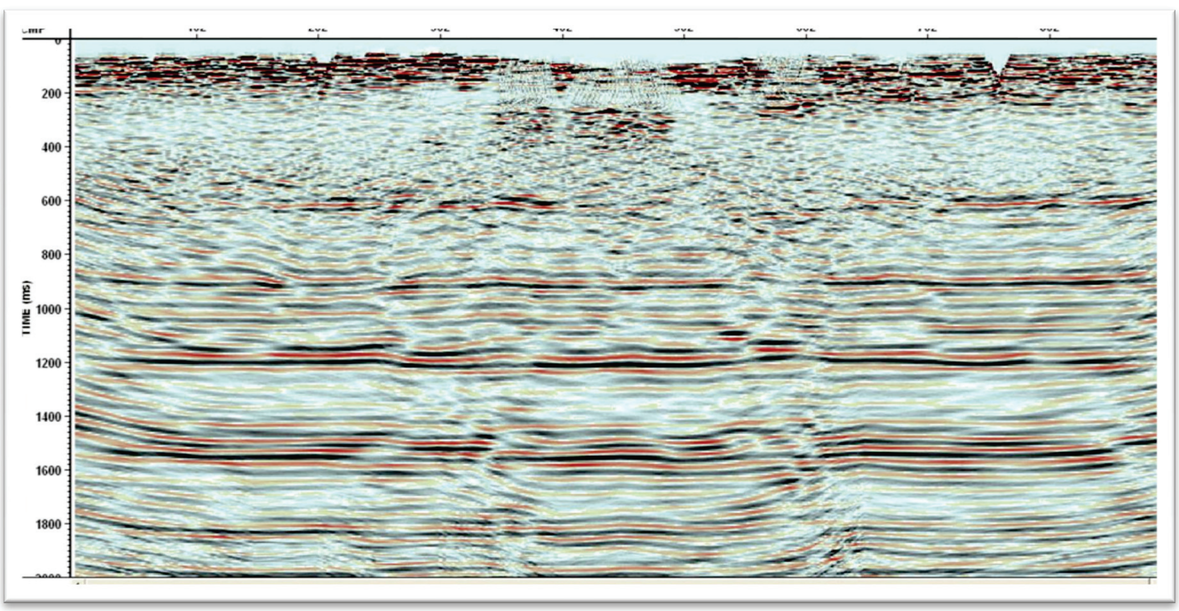

FIG. 22. Kirchhoff PSTM.

The comparison between three migrated sections: one with EOM (Figure 21), the other with Poststack Finite Difference Migration, and the other with Poststack Kirchhoff migration (Figure 23), is that they are look similar; however, the sections with poststack migration applied, show discontinuous reflectors below 1400 milliseconds that are not observed in the EOM section.

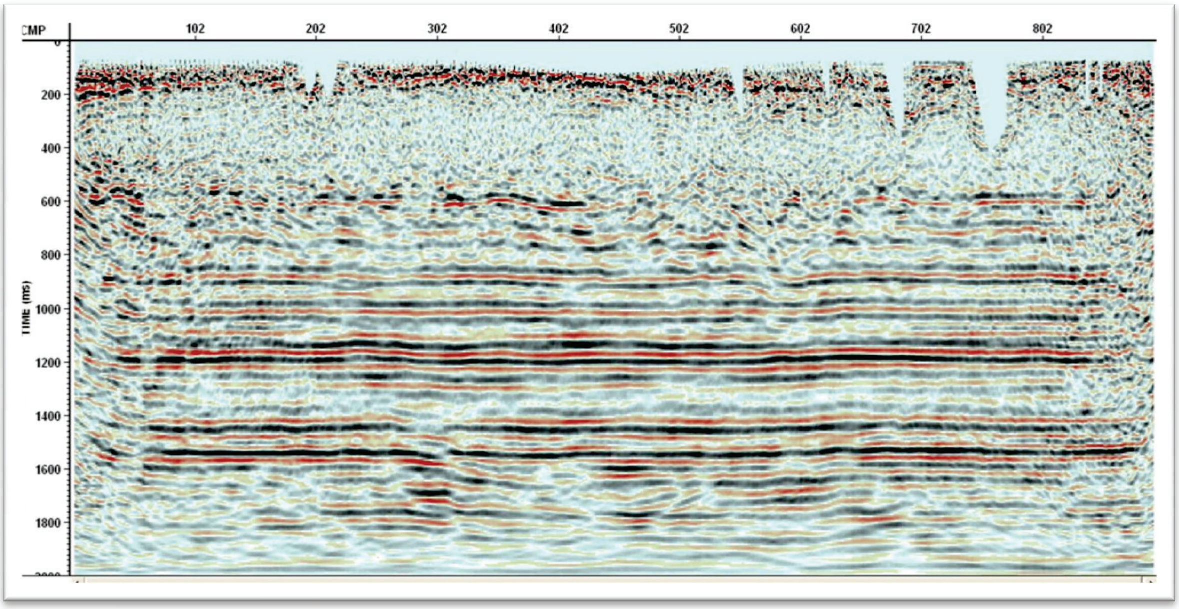

FIG. 23. Finite Difference poststack Migration.

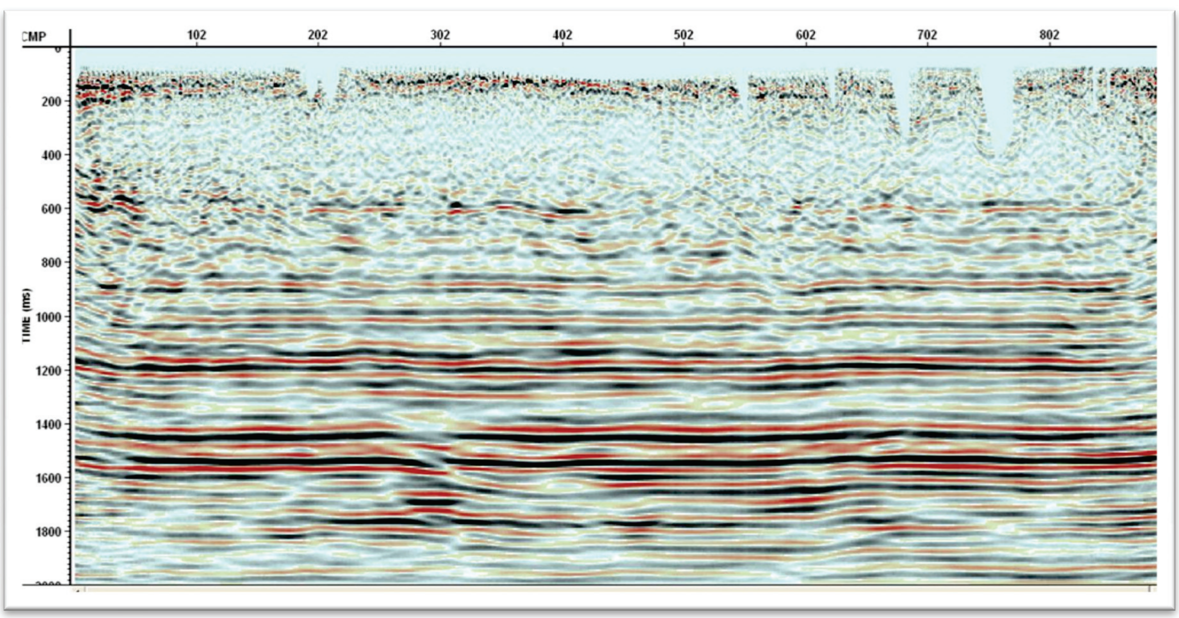

FIG. 24. Kirchhoff poststack Migration.

CONCLUSION

EOM is a method of prestack migration based on the principle of Kirchhoff time migration. This method is simpler, faster flexible and more reliable than conventional methods.

EOM uses an equivalent offset to form CSP gathers. Standard processing of the CSP gather with NMO and stacking completes the prestack migration process.

The CSP gathers have high fold and longer offset than CMP gathers at the same location which allow an improvement of the velocity resolution.

Comparison between EOM and PSTM Kirchhoff show that EOM have improved coherence and interpretability.

ACKNOWLEDGEMENTS

The authors would like to thanks GEDCO for the use of the software VISTA 2D/3D and LANDMARK for the use of the software ProMAX to process the data. Also to Husky Energy, GeoKinetics and Inova for collaborate in the acquisition of Hussar data experiment and all CREWES sponsor and staff for their useful support.

REFERENCES

Bancroft, J. C., Geiger, H.D., Foltinek, D.S., and Wang, S., 1994 Prestack migration by equivalent offsets and CSP gathers: CREWES Research Report, 6, 27.1 -27.18

Bancroft, J., Geiger, H., Wang, S., and Foltinek, D., 1995, Prestack migration by equivalent offset and CSP gathers: an update: CREWES Research Report, 7, 27.1-27.22

Bancroft, J. C., Geiger, H. D., and Margrave, G. F., 1998, The equivalent offset method of prestack time migration: Geophysics, **63**, 2042-2053

Guirigay, T. A., Bancroft, J. C., 2010 Converted wave processing in the EOM domain: CREWES Research Report, 22, 23.1-23.24

Margrave, G. F., 2011, The Hussar Experiment: An investigation into the low-frequency seismic signal band: CREWES News, **23**, N° 1, 6-9